Statistical analysis of Saudi Arabia's COVI 19 spread data using a modified fractional SEIR model

Salem Mubarak Al − Zahrani[a] Fath E.I. Elsmih [b,c] Khalid Salem Al − Zahrani[a] Sayed Saber[c,d]
[a] Faculty of Arts and Science in Almandaq, Al-Baha University, Saudi Arabia.
[b] Department of Mathematics, Faculty of Sciences, Peace University, Sudan
[c] Department of Mathematics, Faculty of Sciences and Arts in Baljurashi, Al-Baha University, Saudi Arabia
[d] Department of Mathematics and Computer Science, Faculty of Science, Beni-Suef University, Egypt.

[*] Corresponding author; E-mail: salem.bb@hotmail.com

Abstract:
This study presents a Covid-19 modified SEIR model that uses a fractional derivative in the sense of Caputo. The existence, uniqueness, and boundedness of the solution of the proposed model are established. The basic reproduction number $\mathcal{R}_0$ is calculated. Using the Lyapunov-LaSalle theorem, local and global stability of free-infected and endemic equilibrium points were established. In addition, perform a sensitivity analysis to determine how parameter changes affect the transmission of early-stage illness. Statistical sensitivity analysis has shown that $\mathcal{R}_0$ is the most sensitive to the density of Covid-19. The Adams-Bashforth Fractional method is used to iteratively calculate the solution of the model.

Keywords: Keywords: Covid-19, mathematical model, SEIR model, fractional calculus, endemic-equilibrium point, stability analysis, Adams-Bashforth fractional method, sensitivity analysis.

Mathematics Subject Classification**:** 92C50, 34K45, 34D20, 92D25

1. Introduction

The outbreak of coronavirus disease (Covid-19) is one of the largest public health problems in the world. Due to its high contagious nature, Covid-19 has caused widespread illness and death in almost every country in the world. Accurately counting the basic reproduction number $\mathcal{R}_0$ helps the decision-makers in implementing efficient control strategies. Meanwhile, on Monday, March 2, 2020, the Saudi Arabian Ministry of Health announced that the first case of a new Covid-19 was detected in citizens arriving at sea from Iran. Statisticians have recently stepped up their efforts to study Covid-19. Various statistical and machine learning-based predictive models have been proposed to estimate the new number of cases in Covid19. Many strategies for developing time-series models have been proposed to predict coronavirus disease in Saudi Arabia, but the applicability of these methods to specific time-series data is more difficult (Huang et al, 2020; Pan et al, 2020; Boldog et al, 2020; Chan et al, 2020; Chen et al, 2020; Chen et al, 2020; Xiong, 2020).

In this study, a modified SEIR epidemiological model is used to estimate $\mathcal{R}_0$ of the new coronavirus disease in Saudi Arabia and to predict how Covid-19 would evolve. Fractional models are a useful tool for modelling real-world situations and have a wide range of applications (Aguila-Camacho et al, 2014; Alshehri et al, 2020; Alshehri et al, 2021; Boukhouima et al, 2017; Choi et al, 2014; Li et al, 2016; Li

et al, 2017; Muhammad and Abdon, 2020; Podlubny, 1999; Saber, 2022; Salem et al). The proposed model is a generalized quadratic nonlinearity for four unknowns' compartments namely, susceptible (S), exposed (E), infected (I), and recovered individuals (R). The problem statement you are solving has been investigated for Covid-19 in several papers see (Ahmad et al, Aletreby et al, 2020; Algaissi et al, 2020; Anderson et al, 2020; Boldog et al, 2020; Chan et al, 2020; Chen et al, 2020; Dur-e-Ahmad and Imran, 2020; Gao et al, 2020; Huang et al, 2020; Khoshnaw et al, 2020; Kuniya, 2020; Linka et al, 2020; Liang, 2020; Liu et al, 2020; Pan et al, 2020; Salem et al; Xiong, 2020; Zhao, 2020). More precisely, the SEIR model of fractional order D^{ν}, $0 < \nu \leq 1$, in the sense of Caputo, is considered and expressed as:

$$\begin{aligned} D^{\nu}S(\tau) &= \kappa - \zeta S(\tau)I(\tau) - \mu S(\tau), \\ D^{\nu}E(\tau) &= \zeta S(\tau)I(\tau) - \varepsilon_1 E(\tau), \\ D^{\nu}I(\tau) &= \gamma E(\tau) - \varepsilon_2 I(\tau), \\ D^{\nu}R(\tau) &= \delta E(\tau) + \alpha I(\tau) - \mu R(\tau), \end{aligned} \tag{1.1}$$

with initial data $S(0) = \mathrm{S}_0, \mathrm{E}(0) = \mathrm{E}_0, \mathrm{I}(0) = \mathrm{I}_0, \mathrm{R}(0) = \mathrm{R}_0$. The biological meanings of the parameters in (1.1) are listed in Table 1.

The purpose of this study was to gain a better understanding of the dynamics of Covid-19's transmission to humans. Based on data on the Covid-19 epidemic in Saudi Arabia, we wanted to identify the best protocols, controls, and strategies to contain the outbreak. In addition, data from Covid-19 in Saudi Arabia were collected from April 5, 2020, to October 2021. As a result, a statistical sensitivity analysis is performed to determine how changes in the parameters affect the transmission of early-stage disease. Statistical sensitivity analysis shows that $\mathcal{R}_0$ is the most sensitive to the density of Covid-19.

2. Properties of Solutions

Denote $\mathbb{R}_+$ the set of all semi-positive real numbers and assume that

$$\Omega = \{(S, E, I, R) \in \mathbb{R}_+^4,\ \mathrm{S} \geq 0,\ \mathrm{E} \geq 0, \mathrm{I} \geq 0,\ \mathrm{R} \geq 0,\ \max(|\mathrm{S}|,\ |\mathrm{E}|,\ |\mathrm{I}|,\ |\mathrm{R}|) \leq \Pi\}.$$

Denote by the Mittag Leffler function $\mathrm{M}_{\nu,1}(\tau)$ as

$$\mathrm{M}_{\nu,1}(\tau) = \sum_{\mathrm{k}=0}^{\infty} \frac{\tau^{\mathrm{k}}}{\Gamma(\nu \mathrm{k} + 1)} > 0,$$

where $\Gamma(\mathrm{z}) = \int_0^{\infty} \mathrm{e}^{-\tau} \tau^{\mathrm{z}-1}\, \mathrm{dt}$ is the Euler gamma function. If $\nu \in \mathbb{R}_+$is a non integer order, the fractional integral $J_{\mathrm{m}}^{\nu}\psi(\tau)$ of the function ψ: $\mathbb{R}_+ \longrightarrow \mathbb{R}$ is defined by

$$J_{\mathrm{m}}^{\nu}\psi(\tau) = \frac{1}{\Gamma(\nu)} \int_{\mathrm{m}}^{\mathrm{t}} (\tau - \theta)^{\nu-1} \psi(\theta)\, \mathrm{d}\theta, \quad \tau \geq \mathrm{m}.$$

Definition 1 (Podlubny, 1999). For $n - 1 < \nu < n, n \in \mathbb{N}$, the Caputo fractional derivative ${}_{\mathrm{m}}^{\nu}D^{\nu}\psi(\tau)$, of order $\nu > 0$, is defined as

$${}_{\mathrm{m}}^{\nu}D^{\nu}\psi(\tau) = \frac{1}{\Gamma(n - \nu)} \int_{\mathrm{m}}^{\mathrm{t}} \frac{\psi^{(n)}(\theta)}{(\tau - \theta)^{\nu+1-\mathrm{n}}}\, \mathrm{d}\theta, \quad \tau \geq \mathrm{m}.$$

Lemma 1. (Li et al, 2017) **, Lemma 3.** If $\mathrm{D}^{\nu}\psi(\tau)$, $0 < \nu < 1$, exists and satisfies

$$\begin{cases} D^{\nu}\psi(\tau) \leq -\omega\,\psi(\tau) + \mu, & for\ all\ \tau, \\ \psi(\tau_0) = \psi_{\tau_0}, \end{cases}$$

for a function $\psi(\tau)$, with $(\omega, \mu) \in \mathbb{R}^2$, $\omega \neq 0$, then

$$\psi(\tau) \leq \left(\psi(\tau_0) - \frac{\mu}{\omega}\right) \mathrm{M}_{\nu,1}(\tau)[-\omega(\tau - \tau_0)^{\nu}] + \frac{\mu}{\omega}.$$

Proposition 1 (Li et al, 2017). With respect to $\tau \geq 0$ and $\sigma_0 = (S(0), E(0), I(0), R(0)) \in \Omega$, the solution $\sigma = (S(\tau), E(\tau), I(\tau), R(\tau)) \in \Omega$ to the fractional order model (1.1) is unique

Proof. Assume that $W(\sigma) = (G_1(\sigma), G_2(\sigma), G_3(\sigma), G_4(\sigma), G_5(\sigma))$ is a mapping with

$$G_1(\sigma) = \kappa - \zeta S(\tau)I(\tau) - \mu S(\tau),$$
$$G_2(\sigma) = \zeta S(\tau)I(\tau) - \varepsilon_1 E(\tau),$$
$$G_3(\sigma) = \gamma E(\tau) - \varepsilon_2 I(\tau),$$
$$G_4(\sigma) = \delta E(\tau) + \alpha I(\tau) - \mu R(\tau).$$

Hence, for $\sigma, \bar{\sigma} \in \Omega$, one obtains

$$\begin{aligned} \|W(\sigma) - W(\bar{\sigma})\| &= |G_1(\sigma) - G_1(\bar{\sigma})| + |G_2(\sigma) - G_2(\bar{\sigma})| + |G_3(\sigma) - G_3(\bar{\sigma})| + |G_4(\sigma) - G_4(\bar{\sigma})| \\ &\leq (\eta I + \mu)|\bar{S} - S| + (\varepsilon_1 + \gamma - \delta)|\bar{E} - E| + (\zeta S - \varepsilon_2 + \alpha)|\bar{I} - I| + \mu|\bar{R} - R| \\ &\leq \ell|\sigma - \bar{\sigma}|, \end{aligned}$$

where

$$\ell = \max\{\eta\Pi + \mu, \varepsilon_1 + \gamma - \delta, \zeta\Pi - \varepsilon_2 + \alpha, \mu\}.$$

Therefore, the Lipschitz condition for $G(\sigma)$ is satisfied. As a result, the solution of (1.1) exists and unique.

Proposition 2 (Li et al, 2017). The fractional-order model (1.1) has non-negative solution.

Proof. One has

$$D^{\nu}S(\tau)|_{S=0} = \kappa > 0,$$
$$D^{\nu}E(\tau)|_{E=0} = \zeta SI > 0,$$
$$D^{\nu}I(\tau)|_{I=0} = \gamma E(\tau) > 0,$$
$$D^{\nu}R(\tau)|_{R=0} = \delta E(\tau) + \alpha I(\tau) > 0.$$

Thus, by using Lemmas 5 and 6 in (Choi et al, 2014), the solution of (1.1) is semi-positive.

Proposition 3 (Li et al, 2017). The fractional-order model (1.1) has uniformly bounded solutions start in

$$\Upsilon = \left\{(S, E, I, R) \in \Omega^{+},\ \ 0 \leq N \leq \frac{\mu}{k}\right\},$$

where $N(\tau) = S(\tau) + E(\tau) + I(\tau) + R(\tau)$.

Proof. The total population $N(\tau)$ at time τ satisfies

$$D^{\nu}N(\tau) = k - \left(\mu S(\tau) + (\varepsilon_1 - \gamma - \delta)E(\tau) + (\varepsilon_2 - \alpha)I(\tau) + \mu R(\tau)\right) \leq k - \omega N(t),$$

where $\omega = min\{\mu,\ \varepsilon_1 - \gamma - \delta, \varepsilon_2 - \alpha, \mu\ \}$. Thus

$$D^{\nu}N(\tau) + \omega N(\tau) \leq k.$$

From Lemma 9 in (Choi et al, 2014),

$$0 \leq N(\tau) \leq N(0)M_{\nu}(-\omega\tau^{\nu}) + \tau^{\nu}M_{\nu,\nu+1}(-\omega\tau^{\nu}),$$

where M_{ν} is the Mittag-Leffer function. Therefore, one obtains:

$$0 \leq N(\tau) \leq \frac{k}{\omega}, \quad \tau \longrightarrow \infty,$$

(see (Boukhouimaet al, 2017) ; Lemma 5 and Corollary 6). Thus, in the region Υ, the solution of (1.1), starting in Ω, is uniformly bounded.

Proposition 4 (Aguila-Camacho et al, 2014**).** Let $y = 0$ be an equilibrium of non-autonomous fractional order system

$$\begin{cases} D^{\nu}y(\tau) = f(\tau, y), \\ y(0) = y_0. \end{cases}$$

Let $\Omega \subseteq R^n$ be the domain containing $y = 0$, and let $L(\tau, y) : [\tau_0, \infty] \times \Omega \to R$ be a continuous differentiable function such that $W_1(x) \leq L(\tau, x) \leq W_2(x)$ and

$$D^{\nu}L(t, x) \leq -W_3(x), \text{ for } \tau \geq 0, y \in \Omega,$$

where $W_1(x)$, $W_2(x)$, $W_3(x)$ are continuous positive functions on Ω and L is Lyapunov candidate function, then $y = 0$ is asymptotically stable globally.

Proposition 5 (Delvari et al, 2012). If $y(t) \in R$ is a continuous differentiable function, then for all $\nu \in (0,1)$,

$$\frac{1}{2}D^{\nu}y^2(\tau) \leq D^{\nu}y(\tau), \quad \text{for any } \tau \geq \tau_0.$$

3 Methods

By constructing the appropriate Lyapunov function, the local and global stability of the free and endemic equilibrium points will be studied. First, calculate the basic reproduction number as follows.

3.1 Computing the basic reproduction number

Let $x = (S, R)^T$ and $y = (E, I)^T$, then we have

$$D^{\nu}y = \mathring{A}(y) - \mathcal{B}(y),$$

where

$$\mathring{A}(y) = \begin{bmatrix} \zeta SI \\ 0 \end{bmatrix}, \quad \mathcal{B}(y) = \begin{bmatrix} \varepsilon_1 E(t) \\ -\gamma E(t) + \varepsilon_2 I(t) \end{bmatrix}.$$

At the infection-free equilibrium point P_0, the Jacobian matrices H and K of the two matrices $\mathring{A}(y)$ and $\mathcal{B}(y)$, are respectively given by

$$H = \begin{bmatrix} 0 & \frac{\zeta k}{\mu} \\ 0 & 0 \end{bmatrix}, \quad K = \begin{bmatrix} \varepsilon_1 & 0 \\ -\gamma & \varepsilon_2 \end{bmatrix}.$$

Therefore

$$K^{-1} = \begin{bmatrix} \frac{1}{\varepsilon_1} & 0 \\ \frac{\gamma}{\varepsilon_1\varepsilon_2} & \frac{1}{\varepsilon_2} \end{bmatrix}.$$

The spectral radius $\rho(H.K^{-1})$ of the matrix $H.K^{-1}$ is given by

$$\rho(H.K^{-1}) = \frac{\zeta\gamma k}{\mu\varepsilon_1\varepsilon_2}.$$

So, $\mathcal{R}_0$ is given by

$$\mathcal{R}_0 = \frac{\zeta\gamma k}{\mu\varepsilon_1\varepsilon_2}.$$

Moreover, on can derive the following

$$\mathcal{R}_0 = \frac{\zeta\gamma k}{\mu\varepsilon_1\varepsilon_2} = \frac{\zeta\gamma k}{\mu(\mu+\alpha)(\mu+\gamma+\delta)}.$$

3.2 Stability analysis of the free equilibrium point

If $I = 0$, one can obtain the infection-free equilibrium point $P_0 = \left(\frac{k}{\mu}, 0,0,0\right)$.

Lemma 2. $P_0 = \left(\frac{k}{\mu}, 0,0,0\right)$ is locall asymptotic stable in Ω If $\mathcal{R}_0 < 1$, and unstable if $\mathcal{R}_0 > 1$.

Proof. The Jacobian matrix $J(P_0)$, at $P_0 = \left(\frac{k}{\mu}, 0,0,0\right)$, for the fractional-order model (1.1) is given by

$$J(P_0) = \begin{bmatrix} -\mu & 0 & -\frac{\zeta k}{\mu} & 0 \\ 0 & -\varepsilon_1 & \frac{\zeta k}{\mu} & 0 \\ 0 & \gamma & -\varepsilon_2 & 0 \\ 0 & \delta & \alpha & -\mu \end{bmatrix},$$

and its characteristic equation is given by

$$(\lambda+\mu)^2\left(\lambda^2 + (\varepsilon_1+\varepsilon_2)\lambda + \varepsilon_1\varepsilon_2 - \frac{\zeta k\gamma}{\mu}\right) = 0. \tag{3.1}$$

From Eq. (3.1), the eigenvalues are: $\lambda_1 = \lambda_2 = -\mu$ and the other values can obtain from the equation

$$\lambda^2 + (\varepsilon_1+\varepsilon_2)\lambda + \varepsilon_1\varepsilon_2 - \frac{\zeta k\gamma}{\mu} = 0. \tag{3.2}$$

Then, $P_0 = \left(\frac{k}{\mu}, 0,0,0\right)$ is stable according to the Routh-Hurwits (Hurwitz, 1964) criterion if and only if all the eigenvalues

are < 0. Obviously, the eigenvalues λ_1, λ_2 are all negatives. Thus, the stability of Eq. (3.2) depends on whether it is $\lambda_3 < 0, \lambda_4 < 0$, or not. If $\mathcal{R}_0 < 1$, λ_3, λ_4, is computed directly, the sufficient stability condition is given by $\mathcal{R}_0 < 1$. That is, the required and adequate condition is $\mathcal{R}_0 < 1$that the system (1.1) is local asymptotic stable at P_0. Otherwise, when $\mathcal{R}_0 > 1$, the system (1.1) is unstable.

Lemma 3. If $\mathcal{R}_0 < 1$, P_0 is global asymptotic stable and unstable if $\mathcal{R}_0 > 1$.
Proof. Construct an effective Lyapunov function as follows:

$$L_1 = \gamma E + \varepsilon_1 I.$$

Then

$$\begin{aligned} D^\nu L_1 &= \gamma D^\nu E + \varepsilon_1 D^\nu I \\ &= (\zeta\gamma S - \varepsilon_1\varepsilon_2) I \\ &\leq (\zeta\gamma S^* - \varepsilon_1\varepsilon_2) I. \end{aligned}$$

Therefore, if $\mathcal{R}_0 < 1$, then $D^\nu L_1 \leq 0$.. In addition, $\{(\mathrm{S}, \mathrm{E}, \mathrm{I}, \mathrm{R}) \in \Omega, D^\nu L_1 \leq 0\}$ is the largest invariant set. Thus, P_0 is asymptotically stable globally by using the invariance principle of LaSalle (LaSalle, 1976).

3.3 Stability analysis of the endemic equilibrium point

For $I^* > 0$, one obtains

$$\begin{aligned} 0 &= \kappa - \zeta S^* I^* - \mu S^*, \\ 0 &= \zeta S^* I^* - \varepsilon_1 E^*, \\ 0 &= \gamma E^* - \varepsilon_2 I^*, \\ 0 &= \delta E^* + \alpha I^* - \mu R^*. \end{aligned}$$

By solving these equations, the unique endemic-equilibrium point is given by: $P^* = (S^*, E^*, I^*, R^*)$, where

$$S^* = \frac{\varepsilon_1\varepsilon_2}{\zeta\gamma}, \qquad E^* = \frac{k\zeta\gamma-\varepsilon_1\varepsilon_2\mu}{\varepsilon_1\zeta\gamma}, \qquad I^* = \frac{\gamma k\zeta-\varepsilon_1\varepsilon_2\mu}{\zeta\varepsilon_1\varepsilon_2}, \qquad R^* = \frac{\zeta\gamma^2\alpha k+\varepsilon_2\delta\zeta\gamma k-\varepsilon_1\varepsilon_2\alpha\gamma\mu-\delta\varepsilon_1\varepsilon_2^2\mu}{\varepsilon_1\varepsilon_2}.$$

Lemma 4. If $\mathcal{R}_0 < 1$, the endemic equilibrium point $P^* = (S^*, E^*, I^*, R^*)$, is local asymptotic stable in Ω.

Proof. The Jacobian matrix $J(P^*)$, at $P^* = (S^*, E^*, I^*, R^*)$, of the fractional order system (1.1) is given by

$$J(P^*) = \begin{bmatrix} -\zeta I^* - \mu & 0 & -\zeta S^* & 0 \\ \zeta I^* & -\varepsilon_1 & \zeta S^* & 0 \\ 0 & \gamma & -\varepsilon_2 & 0 \\ 0 & \delta & \alpha & -\mu \end{bmatrix}.$$

Its characteristic equation

$$(\lambda + \mu)(\ell_1\lambda^3 + \ell_2\lambda^2 + \ell_3\lambda + \ell_4) = 0, \tag{3.3}$$

where

$\ell_1 = 1, \quad \ell_2 = \varepsilon_1 + \varepsilon_2 + \mu + \zeta I^*, \qquad \ell_3 = \varepsilon_1\varepsilon_2 - \gamma\zeta S^* + (\varepsilon_1 + \varepsilon_2)(\mu + \zeta I^*),$

$\ell_4 = (\mu + \zeta I^*)(\varepsilon_1\varepsilon_2 - \gamma\zeta S^*) - \gamma\,\zeta^2 S^* I^*$. Eq. (3.3), gives: $\lambda_1 = -\mu$, and the other values can be obtained from the equation

$$\ell_1\lambda^3 + \ell_2\lambda^2 + \ell_3\lambda + \ell_4 = 0.$$

Based on Routh-Hurwitz conditions (Hurwitz, 1964), one obtains

$$D_1(P^*) = \begin{bmatrix} \ell_1 & \ell_2 \\ \ell_2 & \ell_4 \\ \dfrac{\ell_2\ell_3 - \ell_4\ell_1}{\ell_2} & 0 \\ \ell_4 & 0 \end{bmatrix}.$$

If you make sure that $\frac{\ell_2\ell_3-\ell_4\ell_1}{\ell_2}$ has the same sign as ℓ_3, the three eigenvalues have a negative real part. Because $\ell_1 > 0\,, \ell_2 > 0, \ell_3 > 0, \ell_4 > 0, \frac{\ell_2\ell_3-\ell_4\ell_1}{\ell_2} > 0$ and $\ell_2\ell_3 > \ell_4\ell_1$ hold. This validates the Routh-Hurbitz stability condition and P^* is locally asymptotically stable.

Lemma 5. The unique endemic equilibrium point $P^* = (S^*, E^*, I^*, R^*)$, of the fractional-order model (1.1) is asymptotically stable globally.

Proof. Define the Lyapunov candidate function, as in (Delvari, 2012), as follows.

$$L(S(\tau), E(\tau), I(\tau), R(\tau)) = \frac{1}{2}(S(\tau) - S^*)^2 + \frac{1}{2}(E(\tau) - E^*)^2 + \frac{1}{2}(I(\tau) - I^*)^2 + \frac{1}{2}(R(\tau) - R^*)^2\,.$$

Linearity of Caputo operator gives

$$D^\nu L(S(\tau), E(\tau), I(\tau), R(\tau)) = \frac{1}{2}[D^\nu(S(\tau) - S^*)^2 + D^\nu(E(\tau) - E^*)^2 + D^\nu(I(\tau) - I^*)^2 + D^\nu(R(\tau) - R^*)^2]\,.$$

Applying Proposition 5, one obtains

$$\begin{aligned} D^\nu L(S(\tau), E(\tau), I(\tau), R(\tau)) &\le D^\nu(S(\tau) - S^*) + D^\nu(E(\tau) - E^*) + D^\nu(I(\tau) - I^*) + D^\nu(R(\tau) - R^*) \\ &= \kappa - \mu(S(\tau) - S^*) - (\varepsilon_1 - \gamma - \delta)(E(\tau) - E^*) - (\varepsilon_2 - \alpha)(I(\tau) - I^*) \\ &\quad -\mu(R(\tau) - R^*)\,. \\ &\le \kappa - \mathcal{M}(N(\tau) - N^*), \end{aligned}$$

where

$$\mathcal{M} = \min\{\varepsilon_1 - \gamma - \delta, \varepsilon_2 - \alpha, \mu\},$$

$$N^* = S^* + E^* + I^* + R^*$$

$$= \frac{\varepsilon_1\varepsilon_2}{\zeta\gamma} + \frac{k}{\varepsilon_1} - \frac{\varepsilon_2\mu}{\zeta\gamma} + \frac{\gamma k}{\varepsilon_1\varepsilon_2} - \frac{\mu}{\zeta} + \frac{\alpha\gamma k}{\varepsilon_1\varepsilon_2} + \frac{\delta k}{\varepsilon_1} - \frac{\alpha\mu}{\zeta} - \frac{\delta\varepsilon_2\mu}{\zeta\gamma}.$$

Thus

$$D^{\nu}L(S(\tau),E(\tau),I(\tau),R(\tau)) \leq D^{\nu}(S(\tau)-S^{*}) + D^{\nu}(E(\tau)-E^{*}) + D^{\nu}(I(\tau)-I^{*}) + D^{\nu}(R(\tau)-R^{*})$$
$$= \kappa - \mu(S(\tau)-S^{*}) - (\varepsilon_1 - \gamma - \delta)(E(\tau)-E^{*}) - (\varepsilon_2 - \alpha)(I(\tau)-I^{*})$$
$$-\mu(R(\tau)-R^{*}).$$
$$\leq \kappa - \mathcal{M}(N(\tau)-N^{*}),$$

where

$$\mathrm{V(x)} = \mathcal{M}N(t) - (\kappa + \mathcal{M}N^{*}).$$

Therefore, according to Proposition 4, the unique endemic equilibrium point $P^{*} = (S^{*}, E^{*}, I^{*}, R^{*})$, is asymptotically stable globally.

4. Results

4.1. Sensitivity statistical analysis

Statistical sensitivity analysis used to assess the impact relativity of multiple factors on model stability when data is unknown. The analysis can also determine which parameters are important. Calculate the sensitivity index $\mathcal{R}_0$ of the model parameter using both the local and global methods. Local sensitivity analysis uses the normalized forward sensitivity index $\mathcal{R}_0$. In terms of parameters, the sensitivity index $\mathcal{R}_0$ for $\mathcal{R}_0 < 1$ in the model is:

$$\Gamma_{\phi}^{\mathcal{R}_0} = \frac{\partial \mathcal{R}_0}{\partial \phi} \times \frac{\phi}{\mathcal{R}_0}. \tag{4.1}$$

where ϕ is a value from Table 1. Table 1 lists the sensitivity indices of $\mathcal{R}_0$ obtained using Maple. Since

$$\mathcal{R}_0 = \frac{\zeta\gamma k}{\mu\varepsilon_1\varepsilon_2} = \frac{\zeta\gamma k}{\mu(\mu+\alpha)(\mu+\gamma+\delta)}.$$

Then

$$\frac{\partial \mathcal{R}_0}{\partial \kappa} = \frac{\zeta\gamma}{\mu\varepsilon_1\varepsilon_2} > 0, \quad \frac{\partial \mathcal{R}_0}{\partial \zeta} = \frac{\kappa\gamma}{\mu\varepsilon_1\varepsilon_2} > 0, \quad \frac{\partial \mathcal{R}_0}{\partial \gamma} = \frac{\zeta\kappa}{\mu\varepsilon_1\varepsilon_2} > 0,$$
$$\frac{\partial \mathcal{R}_0}{\partial \mu} = -\frac{\zeta\gamma k}{\mu^2\varepsilon_1\varepsilon_2} < 0, \quad \frac{\partial \mathcal{R}_0}{\partial \varepsilon_1} = -\frac{\zeta\gamma k}{\mu\varepsilon_1^2\varepsilon_2} < 0, \quad \frac{\partial \mathcal{R}_0}{\partial \varepsilon_2} = -\frac{\zeta\gamma k}{\mu\varepsilon_2^2\varepsilon_1} < 0,$$
$$\frac{\partial \mathcal{R}_0}{\partial \delta} = -\frac{\zeta\gamma k}{\mu(\mu+\gamma+\delta)^2(\mu+\alpha)} < 0, \quad \frac{\partial \mathcal{R}_0}{\partial \alpha} = -\frac{\zeta\gamma k}{\mu(\mu+\alpha)^2(\mu+\gamma+\delta)} < 0.$$

Equations (3.1) and (3.2) suggest how to select parameters such that $\mathcal{R}_0 < 1$. Therefore, based on this, we can propose appropriate strategies for controlling and preventing the disease. Lemma 3 suggests that you need to control the parameters like $\mathcal{R}_0 < 1$. The sensitivity index reveals the sensitivity of the variable $\mathcal{R}_0$ to the model parameters. A positive (negative) index indicates that an increase in the parameter value results in an increase (decrease) in the $\mathcal{R}_0$ value. Table 1 shows the sensitivity index for each parameter of model (1.1). Analyze the sensitivity of $\mathcal{R}_0$ by inserting the parameter value into equation (4.1) as follows:

$$\Gamma_{\kappa}^{\mathcal{R}_0} = \frac{\partial \mathcal{R}_0}{\partial \kappa} \times \frac{\kappa}{\mathcal{R}_0} = 1, \quad \Gamma_{\zeta}^{\mathcal{R}_0} = \frac{\partial \mathcal{R}_0}{\partial \zeta} \times \frac{\zeta}{\mathcal{R}_0} = 1, \quad \Gamma_{\gamma}^{\mathcal{R}_0} = \frac{\partial \mathcal{R}_0}{\partial \gamma} \times \frac{\gamma}{\mathcal{R}_0} = 1, \quad \Gamma_{\mu}^{\mathcal{R}_0} = \frac{\partial \mathcal{R}_0}{\partial \mu} \times \frac{\mu}{\mathcal{R}_0} = -1,$$
$$\Gamma_{\varepsilon_1}^{\mathcal{R}_0} = \frac{\partial \mathcal{R}_0}{\partial \varepsilon_1} \times \frac{\varepsilon_1}{\mathcal{R}_0} = -1, \quad \Gamma_{\varepsilon_2}^{\mathcal{R}_0} = \frac{\partial \mathcal{R}_0}{\partial \varepsilon_2} \times \frac{\varepsilon_2}{\mathcal{R}_0} = -1, \quad \Gamma_{\delta}^{\mathcal{R}_0} = \frac{\partial \mathcal{R}_0}{\partial \delta} \times \frac{\delta}{\mathcal{R}_0} = -0.33, \quad \Gamma_{\alpha}^{\mathcal{R}_0} = \frac{\partial \mathcal{R}_0}{\partial \alpha} \times \frac{\alpha}{\mathcal{R}_0} = -0.99.$$

The sensitivity coefficients in Table 1 show that when the parameter values κ, ζ, and γ grow while the other parameter values remain constant, the value of $\mathcal{R}_0$ grows. Because the parameters are positive,

this means that the disease's endemicity is increasing. The value of $\mathcal{R}_0$ decreases as the parameter values μ, ε_1, ε_2, δ, and α are decreased while the rest of the parameter values remain constant. Since the indices exhibit negative indications, this indicates a decrease in disease endemicity. The most sensitive parameters are the infection rate ζ from the susceptible population to the infected population and the confirmed infection rate γ from the exposed population, which includes births per unit time and new inhabitants τ, and $\kappa > 0$ are included.

Table 1. Parameters description for the novel (COVID-19) SEIR model

Parameters	Description	values	Sensitivity Index
κ	Includes new births and new residents per unit time	2300	1
ζ	Transmission rate from susceptible population to infected population	1.18×10^{-9}	1
γ	The duration of the latent period	0.2	1
μ	Natural death rate	3×10^{-5}	-1
δ	Suspected infection period	0.1	-0.33
α	Time spent in the infectious category	0.03	-0.99
ε_1	$\varepsilon_1 = \gamma + \mu + \delta$	0.30003	-1
ε_2	$\varepsilon_2 = \alpha + \mu$	0.03003	-1

4.2 Dynamics of $(S - E - I - R)$ for different values of ν

The fractional order form of the SEIR model (1.1) is derived using the predict-evaluate-correct-evaluate (PECE) method of ABM studied in Diethelm (Diethelm, 1997), Diethelm and Freed (Diethelm and Freed, 1999) Diethelm and Ford (Diethelm and Ford, 2002). Its convergence and accuracy have been discussed in Diethelm and Ford (Diethelm and Ford, 2002). Using a set of parameter values in Table 1, one simulates numerical system (1.1) for different values of fractional order ν to support analytical results (Figs. 1, 2). Consider the following:

$$\begin{aligned} D^{\nu}S(\tau) &= 2300 - 1.18 \times 10^{-9} \times S(\tau) \times I(\tau) - 3 \times 10^{-5} \times S(\tau), \\ D^{\nu}E(\tau) &= 1.18 \times 10^{-9} \times S(\tau) \times I(\tau) - 0.30003 \times E(\tau), \\ D^{\nu}I(\tau) &= 0.2 \times E(\tau) - 0.03003 \times I(\tau), \\ D^{\nu}R(\tau) &= 0.1 \times E(\tau) + 0.03 \times I(\tau) - 3 \times 10^{-5} \times R(\tau), \end{aligned} \tag{4.2}$$

with $S(0) = 34218200, E(0) = 103, I(0) = 157, \mathrm{R}(0) = 100$. For these parameters, $P_0 = (3.3333 \times e^{+09}, 0, 0, 0)$ is asymptomatically stable. According to Lemma 3, P_0 is globally asymptotically stable of system (1.1). The numerical Covid-19 model proposed for different fractional order values ν is simulated to support analytical results and to evaluate control strategy effectiveness numerically. Fig. 1 shows the global stability of the model (4.2) at P_0 using potentially different conditions when $\xi = 0.45 \times 10^{-7}$ (thus $\mathcal{R}_0 = 0.2703 < 1$). The solutions of (4.2) converge to the unique disease-free equilibrium P_0, as predicted. P_0 is asymptotically stable globally, according to (1.1). For smaller orders, the effect of μ is even more pronounced; compare $\nu = 0.7, 0.75, 0.80, 0.85, 0.95$ in

Fig.1 (a), (b) (c), (d). Although the number of infected individuals has decreased significantly for smaller fractional orders, the number of susceptible individuals has increased, as shown in Fig. 1(c).

Global stabilities of endemic model equilibrium (4.2) are illustrated in Fig. 2 using potentially different conditions when $\xi = 0.45 \times 10^{-6}$ (so that $\mathcal{R}_0 = 2.7030 > 1$). The solutions of (4.2) converge towards the unique endemic equilibrium of P^*, as predicted. According to Lemma 5, $P^* = (4.0044 \times e^{+03}, 3.3330 \times e^{+05}, 1.9351 \times e^{+03}, 3.3388e \times e^{+04})$, is global asymptotic stable.

The impact of ν is more pronounced for smaller orders; compare $\nu = 0.7, 0.75, 0.80, 0.85, 0.95\nu = 0.7, 0.75, 0.80, 0.85, 0.95$ in Fig. 2 (c), (d). Although the number of infected individuals has dropped for smaller fractional orders, the number of susceptible individuals also increased, as shown in Fig. 2(c).

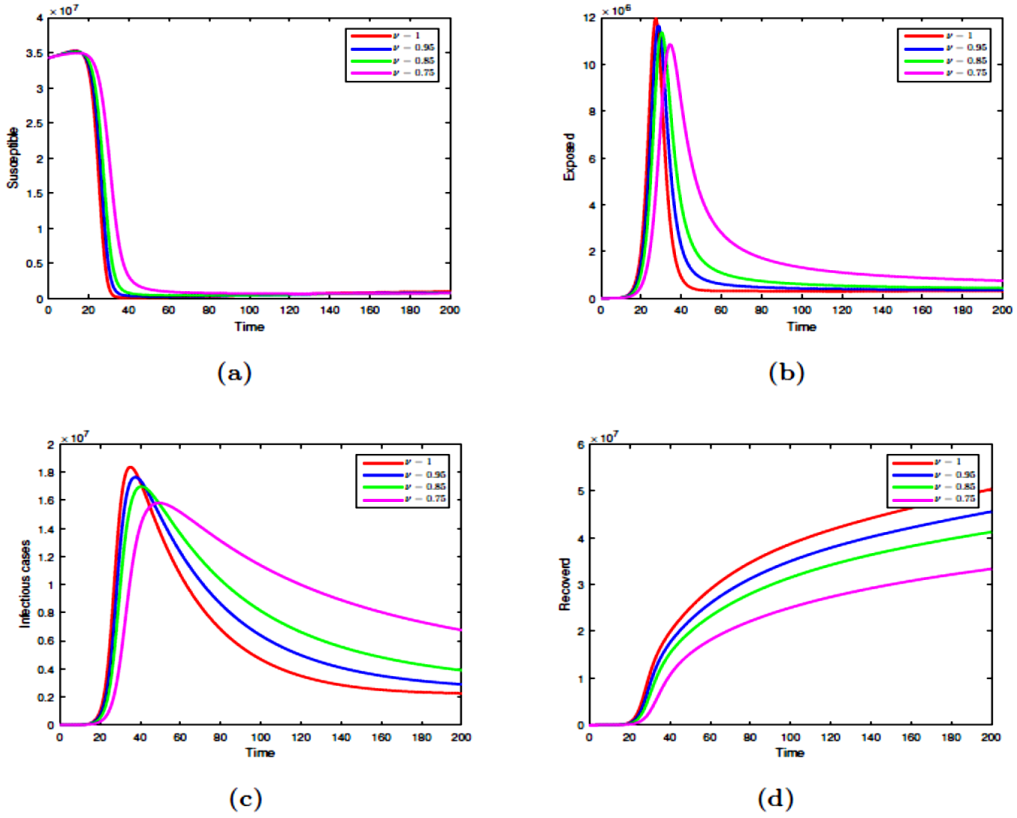

Figure 1. Dynamics of $S(\tau)$, $E(\tau)$, $I(\tau)$, and $R(\tau)$, for different values of ν when $\mathcal{R}_0 = 0.2703$.

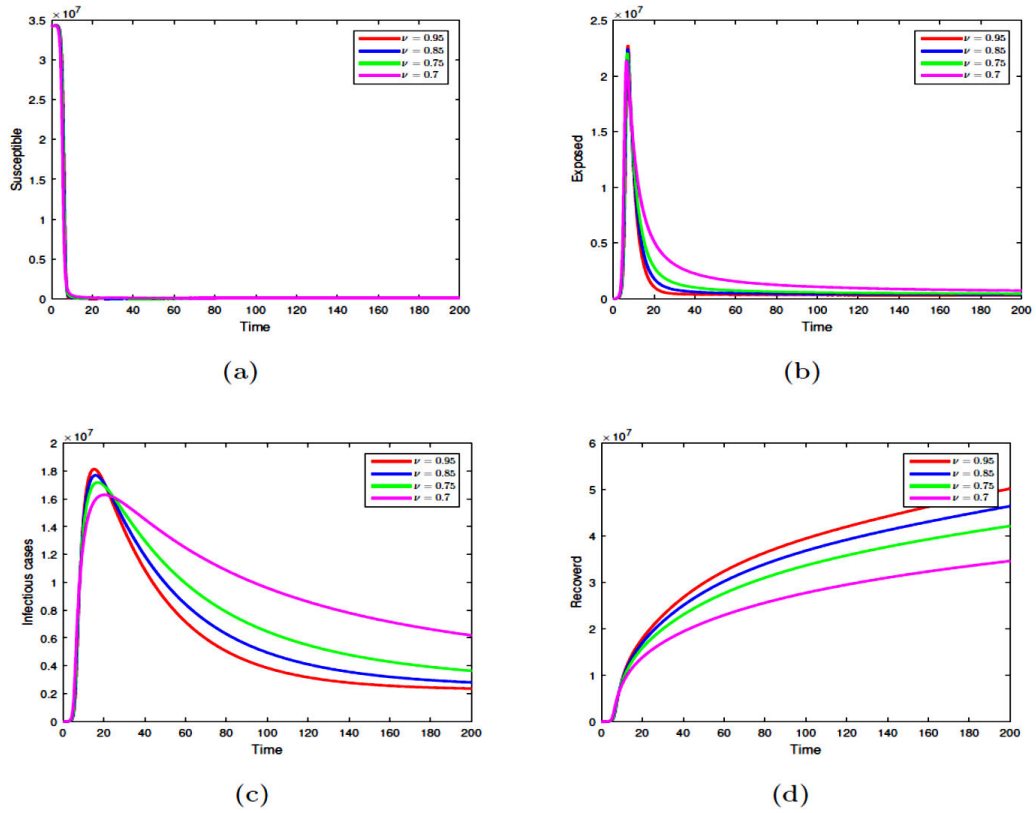

Figure 2. Dynamics of $S(\tau)$, $E(\tau)$, $I(\tau)$, and $R(\tau)$, for different values of ν when $\mathcal{R}_0 = 2.7030$.

4.3 Real situation

We examined evidence of the outbreak of Covid-19 in Saudi Arabia. Covid-19 has spread to Saudi Arabia by March 3, 2020. Covid-19 cases were reported in small numbers until April 1, 2020, when the number of reported cases increased. As a result, it was confirmed that the outbreak of Covid-19 in Saudi Arabia began on April 1, 2020 (Saudi Center for Diseases Prevention and Control, 2020). To find out more about Saudi Arabia's population, mortality, and growth rates, we looked at the Saudi Arabian Ministry of Health tables (Covid-19 in Saudi Arabia, 2020; Saudi Center for Diseases Prevention and Control, 2020; Saudi Ministry of Health, 2020). Figure 3 shows the daily Covid-19 infection curve and total infection timeline curve in Saudi Arabia through October 12, 2021. Figure 3 shows that there were 157 infections on April 1, 2020. Since June 17, 2020, the number of infections has reached 4919. From that date onwards, daily infections decreased until August 5, 2020. Comparing with actual data using the SEIR model, Figure 3 shows the total number of infections that occurred during the same period, starting on August 5, 2020, with 157 infections and ending with 282,824 infections.

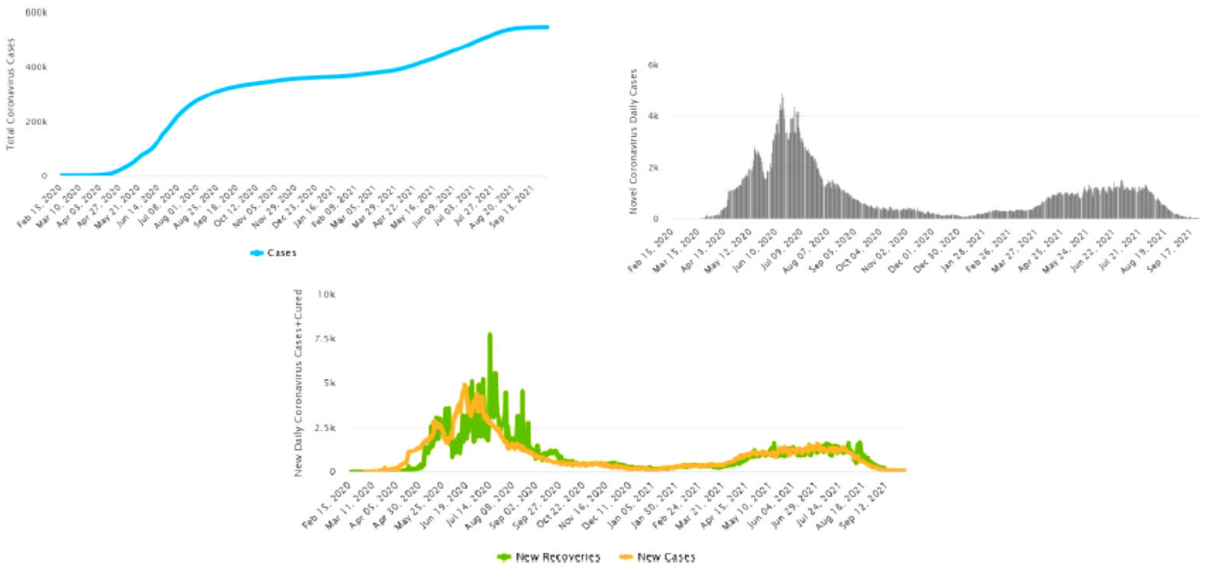

Figure 3. The daily number of cases from April 1, 2020, to October 12, 2021, was calculated based on the SEIR model for actual data from Saudi Arabia (Saudi Center for Diseases Prevention and Control, 2020; Saudi Ministry of Health, 2020).

4.4 Applications

Based on the Nelder-Mead algorithm, the actual data of activity, recovery, and death from Covid-19 in Saudi Arabia are adapted to a modified SEIR model that can predict the future dynamics of the pandemic. We will evaluate some aspects of Covid-19's future dynamics in Saudi Arabia. Validation of the modified fractional SEIR model was divided into two steps. In the first phase, the actual Covid-19 spread data was used between April 1, 2020, and June 17, 2020, when it peaked. As part of the second phase, the actual Covid-19 data was distributed between June 18, 2020, and October 12, 2021. In the first phase, the population of Saudi Arabia was obtained from official data 26 of Saudi Arabia on June 17, 2020. The total number of arrivals and births in Saudi Arabia was about 100,000 per day. Natural deaths occurred at a rate of about $\approx$ 1030 people per day, resulting in $\mu = 3 \times 10^{-5}$. Other parameters were estimated from the actual data (Table 1). As a result of applying the modified SEIR model to the parameter values shown in Table I, we were able to determine the daily infection count. Within the above period, the infection rate of Saudi Arabia from vulnerable people to the infected population was $\xi = 0.45 \times 10^{-6}$. In addition, $\mathcal{R}_0 = 2.7030 > 1$ means that the proportion of susceptible individuals becoming exposed is greater than 1, and the incidence of Covid-19 during this period was not constant. Next, we used an updated SEIR model derived from Saudi Arabian data to explore the new initial state of the system. Table 1 shows the number of infections $I(0) = 4757$, the value of parameter $\xi = 0.45 \times 10^{-7}$, and other parameters. Also, $\mathcal{R}_0 = 0.2703 < 1$. The parameter value at which a sensitive individual became an exposed individual was 1, indicating that the spread of Covid-19 was steady during this period. Figure 3 shows the convergence of the modified SEIR model results with the actual data. From April 1, 2020, to October 12, 2021, the proposed model will be used to estimate daily infections

in Saudi Arabia and compare them to actual data. As a result of applying the modified SEIR model, the result is displayed as a curve following the actual data curve. As a result, the SEIR model results agreed with the actual data. Figure 4 shows the proposed model results and the actual data convergence. The behavior of the two curves is similar and close to each other. In Figures 4 and 5, the results of the modified SEIR model are remarkably close to the actual data, demonstrating the success of the model.

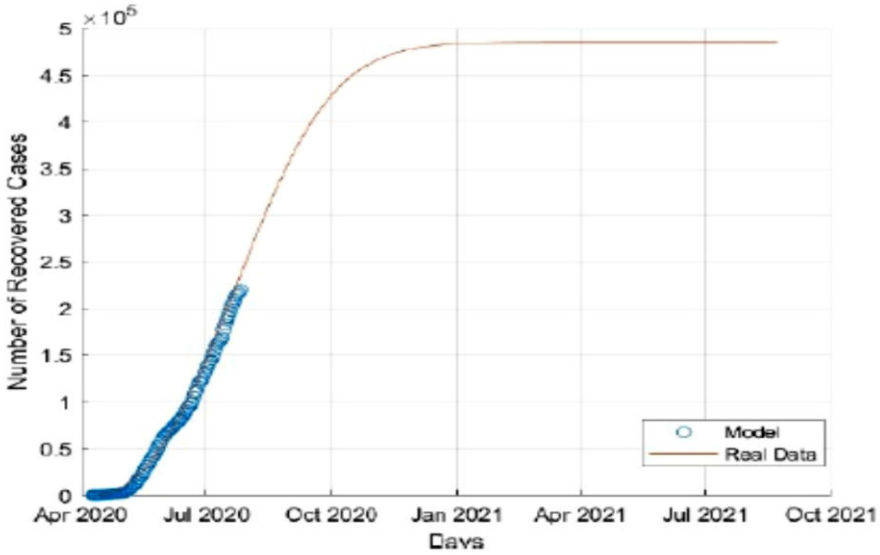

Figure 4. The number of recovery cases based on the SEIR model using actual Saudi Arabia data was calculated between April 1, 2020 and October 12, 2021.

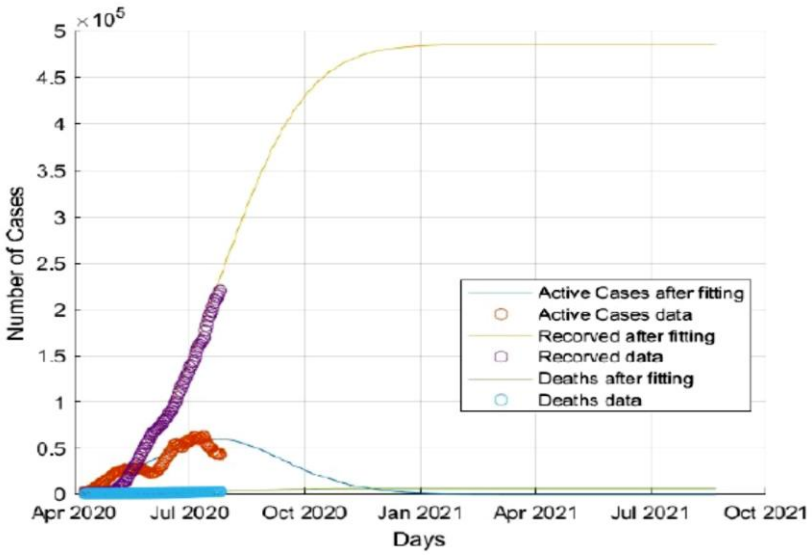

Figure 5. The number of cases based on the SEIR model for actual Saudi Arabia data was calculated between April 1, 2020 and October 12, 2021.

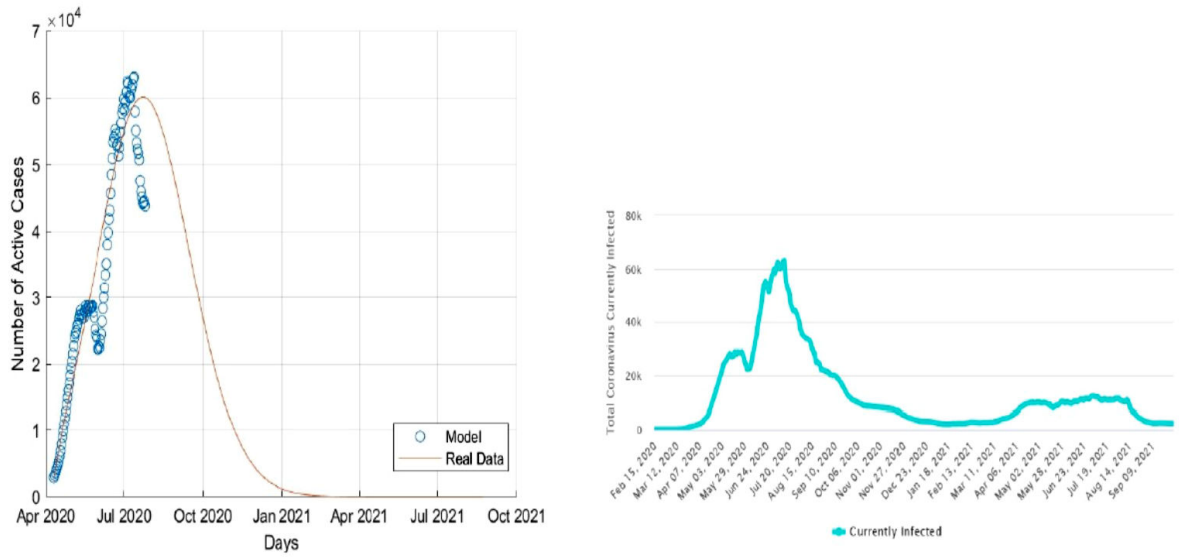

Figure 6. The number of active cases based on the SEIR model for actual Saudi Arabia data was calculated between April 1, 2020 and October 12, 2021 (Saudi Center for Diseases Prevention and Control, 2020; Saudi Ministry of Health, 2020).

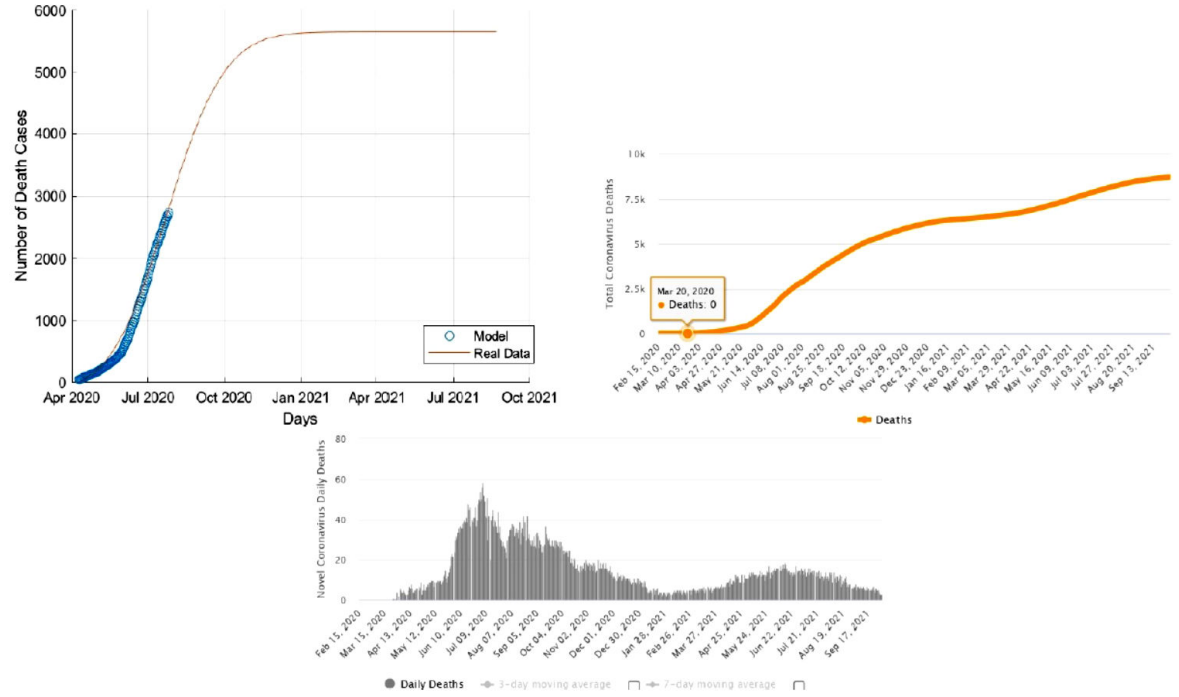

Figure 7. The number of death cases based on the SEIR model for actual Saudi Arabia data was calculated between April 1, 2020 and October 12, 2021 (Saudi Center for Diseases Prevention and Control, 2020; Saudi Ministry of Health, 2020).

4.5 Applying Runge-Kutta method on the case of $\nu = 1$.

Use the ODE technique to solve the initial value problem. Tsit5 () (Tsitoura's 5/4 RungeKutta method) is a standard algorithm suitable for this type of non-rigid ODE. See Figures 8 and 9.

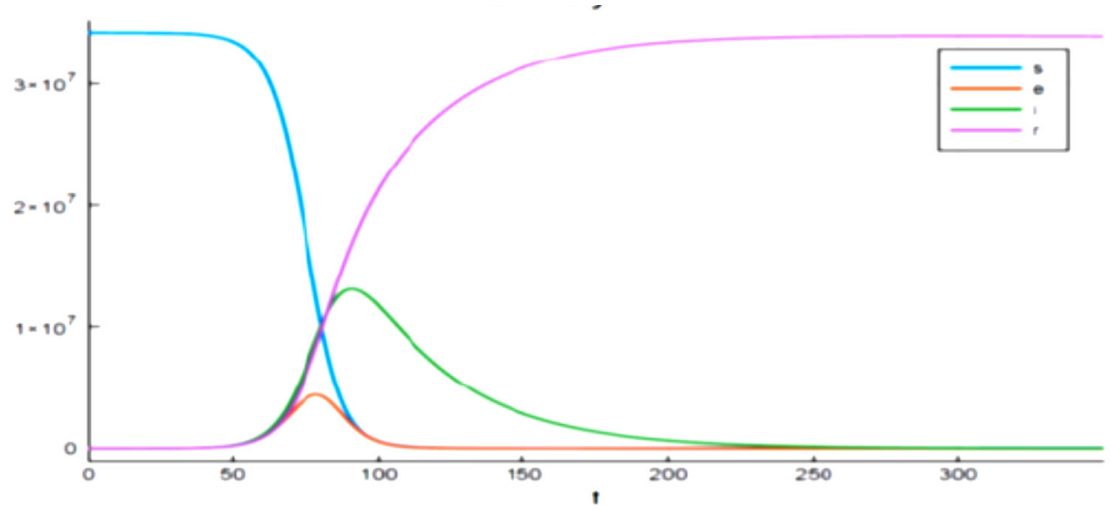

Figure 8. SEIR dynamics for the case of $\boldsymbol{\nu} = \mathbf{1}$.

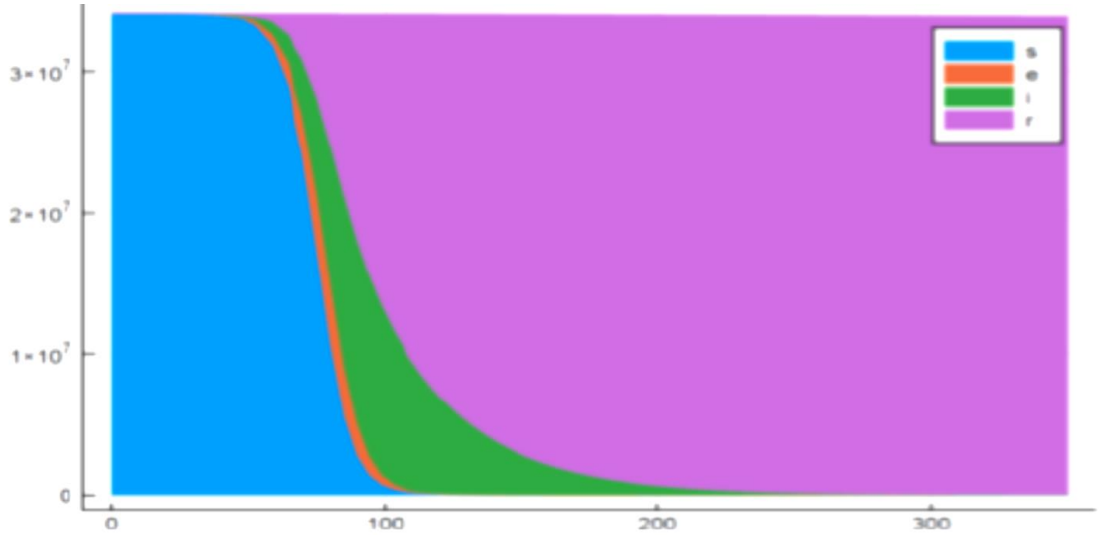

Figure 9. SEIR proportions for the case of $\boldsymbol{\nu} = \mathbf{1}$.

4.6 Experiment 1: Constant case $\mathcal{R}_0$

Consider a situation: $\mathcal{R}_0$ is a constant. Calculate the time course of an infected person under various assumptions of $\mathcal{R}_0$. As expected, low effective infection rates delay the peak of infection, and the peak is lower in the current case.

4.7 Experiment 2: Changing Mitigation

Now imagine a situation where mitigation (social distance, etc.) is gradually progressing. Here, the specification of $\mathcal{R}_0 = \mathcal{R}_0(\tau, r_0 = 3, \eta = 1, r_1 = 1.6)$ as a function of time is as follows:

$$\mathcal{R}_0 = r_0 e^{-\tau\eta} + r_1(1 - e^{-\tau\eta}) .$$

The idea is that $\mathcal{R}_0$ starts at 3 and gradually decreases to 1.6. This is due to the gradual implementation of stricter mitigation measures. The rate at which the limit is imposed is controlled by the parameter η with different rates $\eta = 1/5, 1/10, 1/20, 1/50, 1/100$. The speed or speed imposes limits controlled by the parameter η.

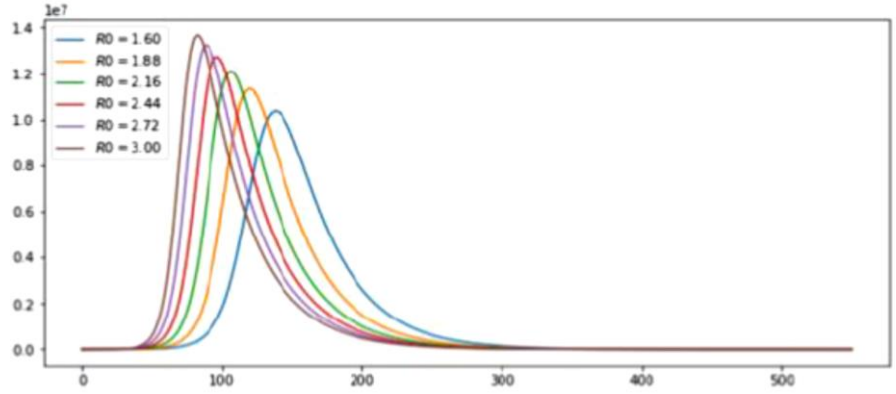

Figure 10. The time path of current cases of infected people under different assumptions of $\mathcal{R}_0$.

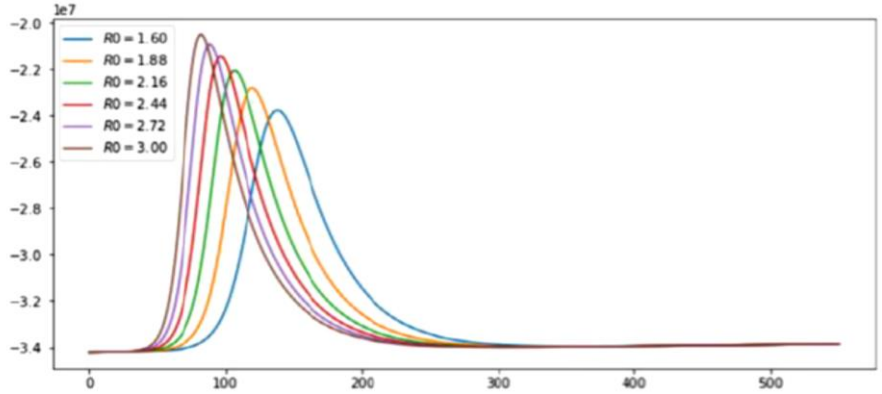

Figure 11. The time path of comulative cases of infected people under different assumptions of $\mathcal{R}_0$.

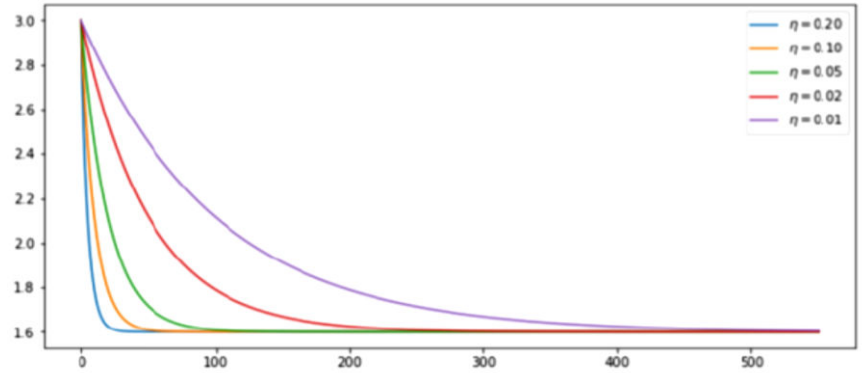

Figure 12. The time path of current cases of infected people under different assumptions of η

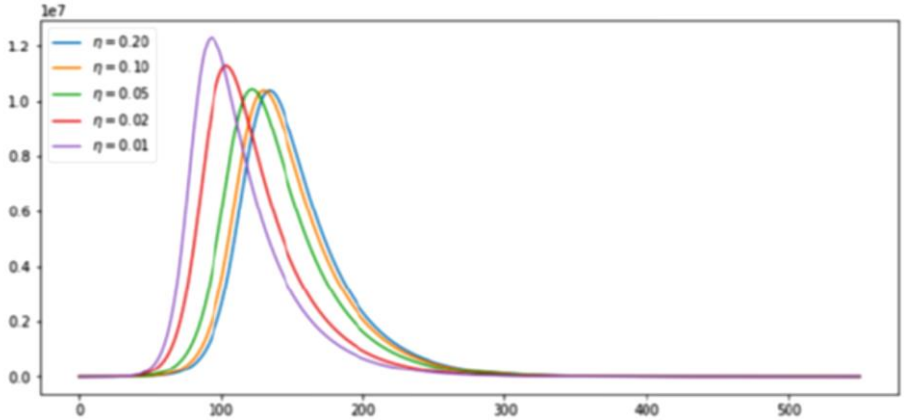

Figure 13. The time path of comulative cases of infected people under different assumptions of η

4.8 Ending Lockdown

Consider the following two mitigation scenarios.

1. $\mathcal{R}_0(\tau) = 0.5$ for 30 days, then $\mathcal{R}_0(\tau) = 0.5$ for the remaining 17 months.

2. $\mathcal{R}_0(\tau) = 0.5$ for 120 days, then $\mathcal{R}_0(\tau) = 2$ for the remaining 14 months.

In both cases, select a large η to concentrate if the quick change of the blocking policy remains feasible.

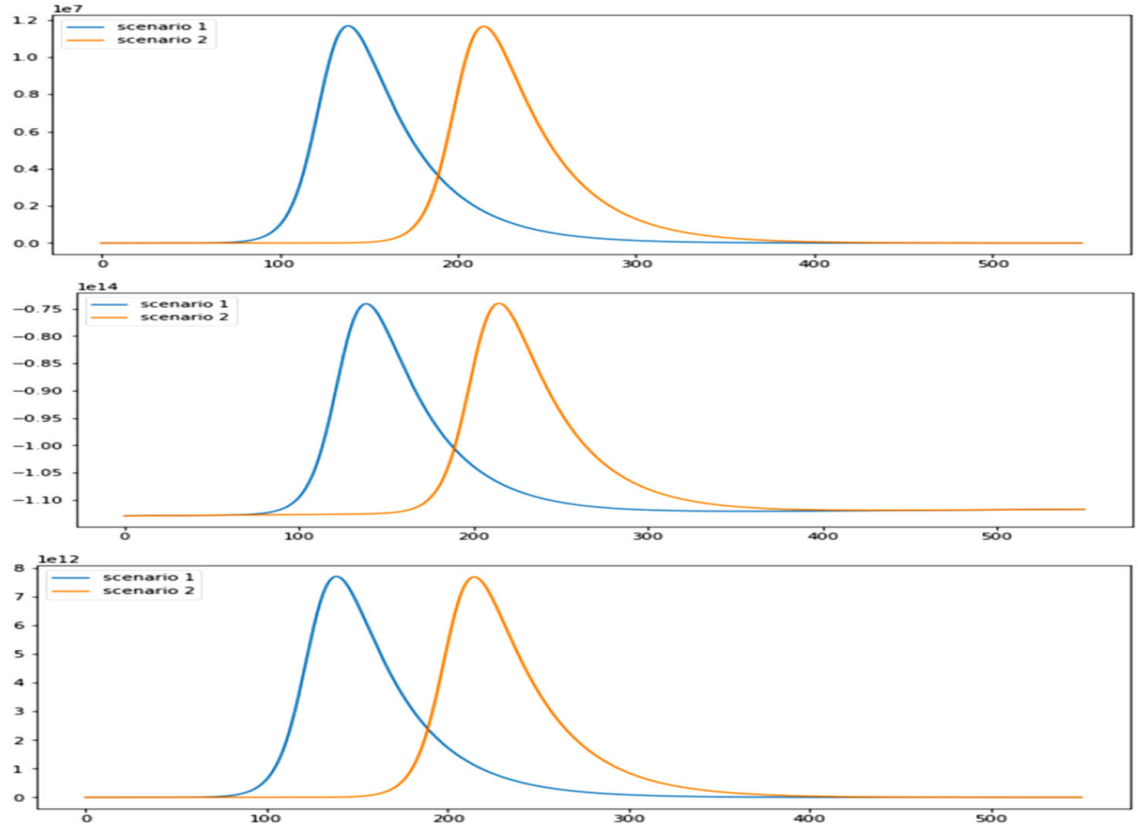

Figure 14. Ending lockdown under mitigation scenarios

5. Discussions

If $\mathcal{R}_0 \leq 1$, the model (1.1) has only a globally stable infection-free equilibrium, meaning that the infection-free equilibrium eventually dies out. Moreover, several strategies are introduced, and the model evolution is drawn up in various cases based on the rate of contact between individuals, which can be effective in minimizing infection. The findings of the fractional SEIR model were compared to the observed outcomes in Saudi Arabia because of Covid-19 spread. Given Covid-19's estimation $\mathcal{R}_0$, reducing the number of contacts in the population is a major step in containing the outbreak. The estimate for $\mathcal{R}_0$ is higher than the estimate for WHO. To achieve the best possible situation to curb the Covid-19 epidemic in Saudi Arabia, we need to begin applying the four key processes and procedures listed below.

1. By evaluating the population with $\xi \leq 0.45 \times 10^{-7}$, reduce the infection rate value from the susceptible population to the infected but undetected population (Prevention, not treatment).

2. To extend the incubation period, reduce the infection rate from individuals confirmed to be infected from the exposed population: $\gamma < 0.2$. This can be achieved by long-term isolation of the infected population from other populations and confinement in a safe place.

3. Increase the transmission rate of recovery from the exposed population $\delta > 0.1$. This approach requires reducing infection detection time by using real-world tools and methods to identify confirmed infections more quickly.

4. Increase the rebound transmission rate of infected populations $\alpha > 0.03$. This can be achieved by reducing the time spent in the infectious category through effective treatment and making vitamins, dietary supplements, and dietary supplements publicly available.

6. Conclusions

We have developed a modified SEIR model. The results of the modified fractional SEIR model were validated using actual Covid-19 spread data from Saudi Arabia. We have shown that a modified fractional SEIR model can be used to analyze epidemic dynamics in Saudi Arabia such as Covid-19. It is important to estimate $\mathcal{R}_0$ of Covid-19 to determine the severity of the pandemic and to design appropriate treatments and responses to protect the population and control the spread of the disease (Covid-19 in Saudi Arabia, 2020). The estimated value of $\mathcal{R}_0$ is important because in the epidemiology of infection, the permeation intensity needs to be reduced by $1 - 1/\mathcal{R}_0$ to eliminate the outbreak. This percentage is 60.0% for $\mathcal{R}_0 = 2.5$, but 68.7% for $\mathcal{R}_0 = 3.2$. Given Covid-19's expected $\mathcal{R}_0$, limiting the number of contacts in a population is a crucial step in combating the epidemic. To counter this pandemic, it may be important to implement programs that extend social distance, ban mass gatherings, restrict transportation, and close schools and facilities. Overall, the predicted $\mathcal{R}_0$ was greater than the WHO estimate.

Availability of data and materials

The dataset used in this study is in the following repository:

1. Saudi Ministry of Health (www.moh.gov.sa/en/Pages/default.aspx),

2. Covid-19 in Saudi Arabia (https://en.wikipedia.org/wiki/Covid-19 pandemic in Saudi Arabia), and

3. The Saudi Center for Disease Prevention and Control is a government organization dedicated to preventing and controlling diseases in Saudi Arabia (https://covid19.cdc.gov.sa/ar/).

Authors' contributions

All authors have read and approved the final manuscript.

Acknowledgment

This research is a part of a project entitled "Using statistics and mathematical modelling to understand infectious disease outbreaks: A case study of the Covid19 epidemic and its impact on the Al-Baha region". This project was funded by the Deanship of Scientific Research, Al-Baha University, KSA (Grant No. 1442/21). The assistance of the deanship is gratefully acknowledged.

References

Aguila-Camacho N., Duarte-Mermoud M. A., Gallegos J. A., 2014. Lyapunov function for fractional; order systems. Commun Nonlinear Sci Numer Simul, 19: 2951–7.

Ahmad, A., Saber, S., Stability Analysis and Numerical Simulations of the Fractional COVID-19 Pandemic Model, Accepted in International Journal of Nonlinear Sciences and Numerical Simulation.

Aletreby W., Alharthy A., Faqihi F., et al., 2020, Dynamics of SARS-CoV-2 outbreak in the Kingdom of Saudi Arabia: a predictive model. Saudi Crit Care J., 4: 79-83.

Algaissi A. A., Alharbi N. K., Hassanain M, Hashem A. M. , 2020, Preparedness and response to COVID-19 in Saudi Arabia: building on MERS experience. J Infect Public Health, 13, 834-838.

Alshehri, M. H., Saber, S., Duraihem F. Z.; "Dynamical analysis of fractional-order of IVGTT glucose–insulin interaction" Accepted in International Journal of Nonlinear Sciences and Numerical Simulation. https://doi.org/10.1515/ijnsns-2020-0201.

Alshehri, M. H., Duraihem, F. Z., Ahmad, A., Saber, S. A, 2021, Caputo (discretization) fractional-order model of glucose-insulin interaction: numerical solution and comparisons with experimental data, J. Taibah Univ. Sci., 15(1) (), 26–36.

Anderson R. M., Heesterbeek H., Klinkenberg D. & Hollingsworth, T.D. , 2020, How will country-based mitigation measures influence the course of the COVID-19 epidemic? COMMENT, 395(10228): 931-934.

Boldog, P., Tekeli, T., Vizi, Z., Dénes, A., Bartha, F., A., Röst, G., Risk, 2020. Assessment of novel coronavirus Covid-19 outbreaks outside China. J Clin Med, 9(2):571.

Boukhouima, A., Hattaf, K., Yousfi, N., 2017. Dynamics of a fractional order HIV infection model with specific functional response and cure rate. Int. J. Differ. Equ., Article ID 8372140.

Chan, JF, Yuan S, Kok KH, To KK, Chu H, Yang J, et al., 2020. A familial cluster of pneumonia associated with the 2019 novel coronavirus indicating person-to-person transmission: a study of a family cluster. Lancet, 395(10223): 514-523.

Chen, N, Zhou M, Dong X, Qu J, Gong F, Han Y, et al., 2020. Epidemiological and clinical characteristics of 99 cases of 2019 novel coronavirus pneumonia in Wuhan, China: a descriptive study. Lancet, 395(10223):507-513.

Chen, TM., Rui, J., Wang, QP. et al. , 2020, A mathematical model for simulating the phase-based transmissibility of a novel coronavirus. Infect Dis Poverty 9, 24.

Choi, S.K., Kang, B., Koo, N., 2014. Stability for Caputo fractional differential systems. Abstr. Appl. Anal., Article ID 631419.

Covid-19 in Saudi Arabia, 2020. https://en.wikipedia.org/wiki/Covid-19 pandemic in Saudi Arabia.

Delvari, H., Baleanu D., Sadati J., 2012. Stability analysis of Caputo fractional-order non- linear systems revisited. J: Nonlinear dynamics. 67:2433–9.

Diethelm, K., 1997. An algorithm for the numerical solution of differential equations of fractional order, Electronic Transactions on Numerical Analysis, 5: 1-6.

Diethelm, K., Freed A. D., 1999. The FracPECE subroutine for the numerical solution of differential equations of fractional order, Proc Forschung und Wissenschaftliches Rechnen, 57-71.

Diethelm, K., Ford, N.J., Freed, A. D., 2002. A predictor-corrector approach for the numerical solution of fractional differential equations}, Nonlinear Dyn., 29: 3–22.

Dur-e-Ahmad M, Imran M ,2020, Transmission dynamics model of coronavirus COVID-19 for the outbreak in most affected countries of the world. Int. J. Interact Multimed Artif Intell. 6: 7-10.

Gao W., Veeresha P., Baskonus H.M., Prakasha D., Kumar P. , 2020, A new study of unreported cases of 2019-nCoV epidemic outbreaks. Chaos Solitons Fractals. 138: 109929.

Huang, C., Wang, Y., Li, X., Ren, L., Zhao, J., Hu, Y., et al., 2020. Clinical features of patients infected with 2019 novel coronavirus in Wuhan, China. Lancet, 395(10223): 497-506.

Hurwitz, A., 1964. On the conditions under which an equation has only roots with negative real parts, in Selected Papers on Mathematical Trends in Control Theory, eds. R. T. Ballman et al. (Dover, New York), 70–82.

Khoshnaw S.H., Shahzad M., Ali M., Sultan F. , 2020, A quantitative and qualitative analysis of the COVID-19 pandemic model. Chaos Solitons Fractals. 138:109932.

Kuniya T. , 2020, Prediction of the epidemic peak of coronavirus disease in Japan, J. Clin. Med. 9(3), 789.

LaSalle J. P., 1976. The stability of dynamics systems. SIAM Philadelphia: PA.

Li, H., Zhang, L., Hu, C., Jiang, Y., Teng, Z., 2016. Dynamical analysis of a fractional-order predator-prey model incorporating a prey refuge. J. Appl. Math. Comput. 54, 435-449.

Linka K, Peirlinck M, Sahli Costabal F, Kuhl E , 2020, Outbreak dynamics of COVID-19 in Europe and the effect of travel restrictions. Comput Methods Biomech Biomed Engin. 11: 710-717.

Liang K. , 2020, Mathematical model of infection kinetics and its analysis for COVID-19, SARS and MERS. Infect Genet Evol. 82: 104306.

Li, H., Zhang, L., Hu, C., Jiang, Y., Teng, Z., 2017. Dynamical analysis of a fractional-order predator-prey model incorporating a prey refuge, J. Appl. Math. Comput. 54: pp. 435–449.

Liu Z, Magal P, Seydi O, Webb G. , 2020, Understanding unreported cases in the COVID-19 epidemic outbreak in Wuhan, China, and the importance of major public health interventions. Biology (Basel) 9(3):50.

Muhammad Altaf Khan, Abdon Atangana , 2020, Modeling the dynamics of novel coronavirus

(2019-nCov) with fractional derivative, Alexandria Engineering Journal, 59(4), 2379-2389.

Pan, F., Ye, T., Sun, P., Gui, S., Liang, B., Li, L., et al., 2020. Time course of lung changes on chest CT during recovery from 2019 novel coronavirus (Covid-19) pneumonia. Radiology, 295(3): 715-721.

Podlubny, I., 1999. Fractional Differential Equations, Academic Press, New York, NY, USA.

Saber, S., Azza, M., Alghamdi, Ghada Elkarim, Khulud, M., Alshehri, 2022. Mathematical Modelling and optimal control of pneumonia disease in sheep and goats in Al-Baha region with cost-effective strategies. AIMS Mathematics, 7(7): 12011-12049. doi: 10.3934/math.2022669

Salem Mubarak Al-Zahrani, Fath E. I. Elsmih, Kaled Salem Al-Zahrani, Sayed S., A fractional order SITR model for forecasting of transmission of COVID-19: Sensitivity Statistical Analysis, Accepted in Malaysian Journal of Mathematical Sciences (MJMS).

Saudi Center for Diseases Prevention and Control, 2020. https://covid19.cdc.gov.sa/ar/daily-updates-ar.

Saudi Ministry of Health, 2020. https://www.moh.gov.sa/en/Pages/default.aspx.

Xiong, H. Yan, 2020. "Simulating the infected population and spread trend of 2019-ncov under different policy by SEIR model". medRxiv.

Zhao S, Musa SS, Lin Q, Ran J, Yang G, Wang W, et al. , 2020, Estimating the unreported number of novel coronavirus (2019-nCoV) cases in China in the first half of January 2020: a data-driven Modelling analysis of the early outbreak. J. Clin. Med. 9(2), 388.